Kolmogorov Turbulence Defeated by Anderson Localization for a Bose-Einstein Condensate in a Sinai-Oscillator Trap

Leonardo Ermann,[1,2] Eduardo Vergini,[1] and Dima L. Shepelyansky[3]
[1]*Departamento de Física, Gerencia de Investigación y Aplicaciones, Comisión Nacional de Energía Atómica. Av. del Libertador 8250, 1429 Buenos Aires, Argentina*
[2]*CONICET, Godoy Cruz 2290 (C1425FQB) CABA, Argentina*
[3]*Laboratoire de Physique Théorique, IRSAMC, Université de Toulouse, CNRS, UPS, 31062 Toulouse, France*
(Received 21 March 2017; published 2 August 2017)

We study the dynamics of a Bose-Einstein condensate in a Sinai-oscillator trap under a monochromatic driving force. Such a trap is formed by a harmonic potential and a repulsive disk located in the center vicinity corresponding to the first experiments of condensate formation by Ketterle and co-workers in 1995. We allow that the external driving allows us to model the regime of weak wave turbulence with the Kolmogorov energy flow from low to high energies. We show that in a certain regime of weak driving and weak nonlinearity such a turbulent energy flow is defeated by the Anderson localization that leads to localization of energy on low energy modes. This is in a drastic contrast to the random phase approximation leading to energy flow to high modes. A critical threshold is determined above which the turbulent flow to high energies becomes possible. We argue that this phenomenon can be studied with ultracold atoms in magneto-optical traps.

DOI: 10.1103/PhysRevLett.119.054103

The Kolmogorov turbulence [1,2] is based on a concept of energy flow from large spacial scales, where an energy is pumped by an external force, to small scales where it is absorbed by dissipation. As a result a polynomial energy distribution over wave modes has been obtained from scaling arguments for hydrodynamics turbulence [1,2]. Later, the theory of weak turbulence, based on diagrammatic techniques and the kinetic equation, demonstrated the emergence of polynomial distributions for various types of weakly interacting nonlinear waves [3–5]. However, this theory is based on a fundamental hypothesis directly stated in the seminal work of Zhakharov and Finonenko: "In the theory of weak turbulence nonlinearity of waves is assumed to be small; this enables us, using the hypothesis of the random nature of the phase of individual waves, to obtain the kinetic equation for the mean square of the wave amplitudes." Nevertheless, the dynamical equations for waves do not involve random phase approximation (RPA) and, hence, the whole concept of energy flow from large to small scales remains open as we discuss below.

Indeed, it is known that in a random media with a fixed potential landscape the phenomenon of Anderson localization [6] breaks a diffusive spreading of probability in space due to quantum interference effects. Even if the underline classical dynamics of particles produces an unlimited spreading. In this respect, the Anderson localization has been observed for a large variety of linear waves in various physical systems [7]. A similar phenomenon appears also for quantum systems in a periodically driven *ac* field with a quantum dynamical localization in energy and number of absorbed photons [8–12]. This dynamical localization in energy has been observed in experiments with Rydberg atoms in a microwave field [12,13] and cold atoms in driven optical lattices [14,15]. Thus, in the localized phase the periodic driving is not able to pump energy to the system even if the classical dynamics is chaotic with a diffusive spreading in energy.

Of course, the Anderson localization takes place for linear waves. The question about its robustness with respect to a weak nonlinearity attracted recently a significant interest of the nonlinear science community [16–20] with the first experiments performed in nonlinear media and optical lattices [21,22]. These studies show that below a certain threshold the Anderson localization remains robust with respect to a weak nonlinearity, while above the threshold a subdiffusive spearing over the whole system size takes place. However, the studies are done for conservative systems without external energy pumping. The numerical simulations for a simple model of the kicked nonlinear Schrödinger equation on a ring gave indications that an energy flow to high energies is stopped by the Anderson localization for a weak nonlinearity [23], but such a model is rather far from real experimental possibilities with nonlinear media or cold atoms.

Here we consider an example of a finite realistic system showing that there is a regime where RPA is not valid and thus instead of energy flow to high energy modes (produced by noisy RPA phases), we obtain an evolution bounded to finite energies. The system represents a Bose-Einstein condensate (BEC) of cold atoms captured in a Sinai-oscillator trap under a monochromatic force. It represents a harmonic trap with a repulsive potential in a

vicinity of the trap center. In fact, a similar system in three dimensions (3D) had been used for a pioneering realization of BEC reported in Ref. [24] (see also Refs. [25,26]). In this experiment a repulsive potential is created by tightly focusing an intense blue-detuned laser that generates a repulsive optical plug bunging a hole in a center of magnetic trap where nonadiabatic spin flips lead to a loss of atoms. This repulsive potential can be well approximated by a rigid disk that creates scattering of atoms and instability of their classical dynamics. In two dimensions (2D) with a harmonic potential replaced by rigid rectangular walls the system represents the well-known Sinai billiard where the mathematical results guarantee that the whole system phase space is chaotic with a positive Kolmogorov entropy [27]. Recently, it was shown that the classical phase space remains practically fully chaotic if the rigid walls are replaced by a harmonic potential which is much more suitable for BEC experiments [28]. The corresponding quantum system is characterized by the level spacing statistics of random matrix theory [29] satisfying the Bohigas-Giannoni-Schmit conjecture [30] and thus belonging to the systems of quantum chaos [31].

The effects of nonlinearity for BEC evolution in a Sinai-oscillator trap have been studied in Ref. [28] in the frame of the Gross-Pitaevskii equation (GPE) [32]. Reference [28] shows that for weak nonlinearity the dynamics of linear modes remains quasi-integrable, while above a certain threshold there is onset of dynamical thermalization leading to the usual Bose-Einstein distribution [33] over energies of linear eigenmodes. By including a monochromatic driving force the energy grows diffusively and probability transfer to high energy modes, typical for the Kolmogorov turbulence, appears. Here we show that there is a regime where such an energy transfer to waves with high wave vectors is suppressed by dynamical localization, in a similar way to the Anderson localization in disordered solids.

We note that the Kolmogorov turbulence for BEC in 2D rectangular and 3D cubic billiards has been studied numerically in Refs. [34,35]. However, the integrable shape of these billiards does not allow us to realize a generic case of random matrix spectrum of linear modes typical for our billiard belonging to the class of quantum chaos systems [31].

For our model, the classical dynamics and quantum evolution in the absence of interactions are described by the Hamiltonian

$$H = \frac{p_x^2 + p_y^2}{2m} + m\frac{\omega_x^2 x^2 + \omega_y^2 y^2}{2} + V_d(x,y) + fx\sin\omega t. \tag{1}$$

Here, the first two terms describe the 2D oscillator with frequencies ω_x, ω_y, the third term represents the potential of rigid disk of radius r_d, and the last term gives a driven monochromatic field of amplitude f. Here we fixed the mass $m = 1$, frequencies $\omega_x = 1$, $\omega_y = \sqrt{2}$, $\omega = (1+\sqrt{5})$, and disk radius $r_d = 1$. The disk center is placed at $(x_d, y_d) = (-1/2, -1/2)$ so that the disk bangs a hole in a center vicinity as was the case in the experiments [24]. In the quantum case one has the usual commutator relations $[\hat{p}_x, \hat{x}] = [\hat{p}_y, \hat{y}] = -i\hbar$ with $\hbar = 1$ for dimensional units.

The BEC evolution in the Sinai oscillator trap is described by the GPE, which reads,

$$i\hbar\frac{\partial\psi(x,y,t)}{\partial t} = \hat{H}\psi(x,y,t) + \beta|\psi(x,y,t)|^2\psi(x,y,t), \tag{2}$$

where β describes nonlinear interactions for BEC. Here we use the same Sinai oscillator parameters as in Ref. [28] with normalization $\int |\psi|^2 dxdy = 1$. The numerical integration of Eq. (2) is done in the same way as in Refs. [11,28] with a Trotter time step ($\Delta t = 0.005$) evolution for the noninteracting part of $\hat{H}$ followed by the nonlinear term contribution. Of course, the GPE gives only an approximate description of many-body quantum evolution but as in Refs. [34,35] we restrict our studies by this approximation.

The results for energy E growth with time for classical dynamics (1) are shown in Fig. 1. The energy E and its dispersion σ are steadily growing with time. We expect that at large times the energy increases diffusively with a rate $(\Delta E)^2/t = D \approx Cf^2\omega_x{}^2 r_d\sqrt{E}/\omega^2$, assuming that $\omega_x \sim \omega_y \sim \omega_x$. The data of Fig. 1 give us $C \approx 0.5$ at $t = 10^3$.

We note that the estimate for D comes from the fact that an oscillating velocity component $v_{\rm osc} = f\cos(\omega t)/\omega$ gives a velocity change at disk collision (like with

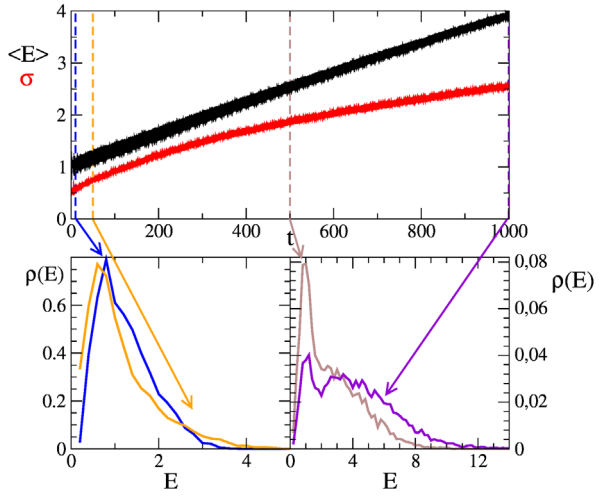

FIG. 1. Classical time evolution of average energy $\langle E\rangle$ and its standard deviation σ for $f = 0.4$. The data are obtained from 10^4 trajectories with random initial conditions at $\langle E\rangle = 1$ and $\sigma = 0.5$. Top panel: $\langle E(t)\rangle$ and $\sigma(t)$ are shown by black and red (gray) curves, respectively. Bottom panels show probability distribution of trajectories $\rho(E,t)$ for (a) $t = 10, 50$ [blue (black), orange (gray) curves] and (b) $t = 500, 1000$ [yellow (gray), violet (black) curves]. Vertical dashed lines in main panels mark snapshot times corresponding to bottom panels.

oscillating wall) $\Delta v_x = 2v_{\rm osc}$ and an energy change $\Delta E \approx v_x \Delta v_x$, so that the diffusion is $D \sim (\Delta E)^2/t_c$, where an average time between collisions t_c is defined from the ergodicity relation $\Delta t_c/t_c \sim r_d{}^2\omega_x{}^2/E$ of ratio of disk area and area of chaotic motion at energy E, where $\Delta t_c \sim r_d/E^{1/2}$; thus at large times $E \propto t^{2/3}$. The fit for $E \sim \sigma \propto t^{\alpha}$ in Fig. 1 gives $\alpha = 0.98 \pm 0.06$ (for E) and 0.58 ± 0.08 (for σ) being comparable to the theoretical value $\alpha = 2/3$. We attributed a deviation from theory to not sufficiently large amplitude of motion $\sqrt{2E}/\omega_x$ required for t_c expression at reached energies.

We also introduce cells of finite energy size δE and determine the probability distribution ρ_k over k energy cells counting a relative number of trajectories inside each one. The results of Fig. 1 show that the width of probability distribution $\rho(E)$ is growing in time corresponding to the increase of E.

The situation is drastically different in the quantum case at $\beta = 0$. Here, at small f, the dynamical localization leads to a complete suppression of energy E and average mode number $M = \sum_k k\rho_k$ growth with their restricted oscillations in time (see Fig. 2). The probability distribution ρ_k over eigenstates ψ_k with eigenenergies E_k of Eq. (1) (for stationary case $f = 0$) is shown in Fig. 3. For small $f < f_c$, on average there is a clear exponential decay of probability $\rho_k \propto \exp(-2E_k/\omega\ell_\phi)$ with a number of absorbed photons $N_\phi = E_k/\omega$ and a photonic localization length ℓ_ϕ. Such a localization decay is similar to those discussed for atoms [12,13] and quantum dots [11] in a microwave field. However, above a certain f_c, e.g., at $f = 2; 3$, we obtain delocalized probabilities ρ_k with a flat plateau distribution at high energies.

According to the theory of dynamical localization described in Refs. [11,12,36] we have $\ell_\phi \approx 2\pi(D/\omega^2)\rho_c$, where $\rho_c = dk/dE_k$ is the density of E_k states. According to Ref. [28] we have $k \approx E^2/2\sqrt{2}$ and $\rho_c \approx E/\sqrt{2}$. With the above expression for the classical diffusion in energy D we obtain $\ell_\phi \approx 2f^2\omega_x{}^2E^{3/2}/\omega^4$. Similar to the quantum chaos model [36] we have ℓ_ϕ significantly growing with the number of absorbed photons N_ϕ so that the delocalization of quantum chaos takes place at $\ell_\phi > N_\phi$. As in Ref. [36] this leads to a delocalization above a certain border $f > f_c$ with a flat probability distribution on high energies as it is seen in Fig. 3. This gives the delocalization border for quantum states: $f_c r_d/\hbar\omega_x \approx 0.7(\omega/\omega_x)^{3/2} \approx 4$ for the initial ground state at $E \approx \hbar\omega_x = 1$ and $\omega \approx 3.2$. The data for M in Fig. 3 give the critical value $f_c \approx 1.5$ being somewhat smaller than the value given by the above estimate. We attribute this difference to the fact that the above estimate for D, and, hence, for ℓ_ϕ, is valid in the limit of large spacial oscillations being larger than r_d. The delocalization transition at $f > f_c$ is similar to the Anderson transition, or metal-insulator transition, in disordered systems [6,7].

The results for $\beta > 0$ are presented in Figs. 2, 4. For $f = 0.4$, when the steady-state probability is well localized at $\beta = 0$, they clearly show that at $\beta = 1.5$ there is no growth of energy E and mode number M. Thus, there is no

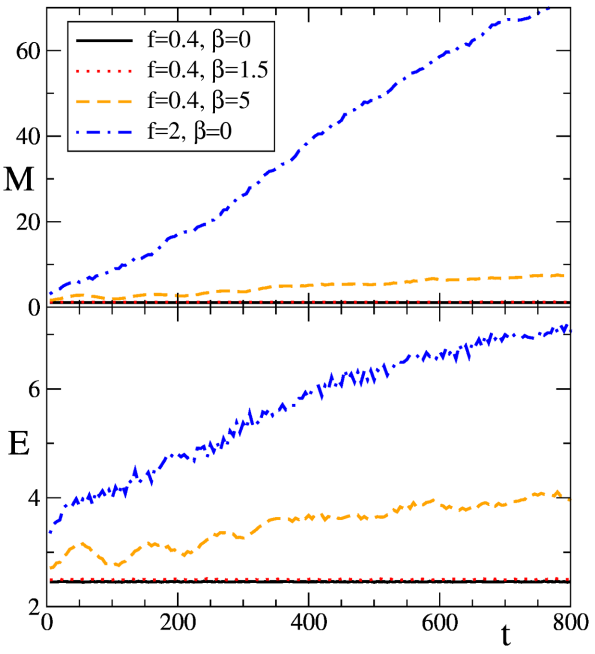

FIG. 2. Time evolution of M (top panel) and energy E (bottom panel) for GPE (2) averaged over time intervals $\Delta t = 1$. The initial state is the ground state of (2) at $\beta = 0$, $f = 0$ [see Fig. 5(a) in Ref. [28]]. Both panels show the cases of $f = 0.4, \beta = 0$ (black solid lines), $f = 0.4$, $\beta = 1.5$ [red (gray) dotted lines], $f = 0.4$, $\beta = 5$ [orange(gray) dashed lines], $f = 2, \beta = 0$ [blue (gray) dot-dashed lines].

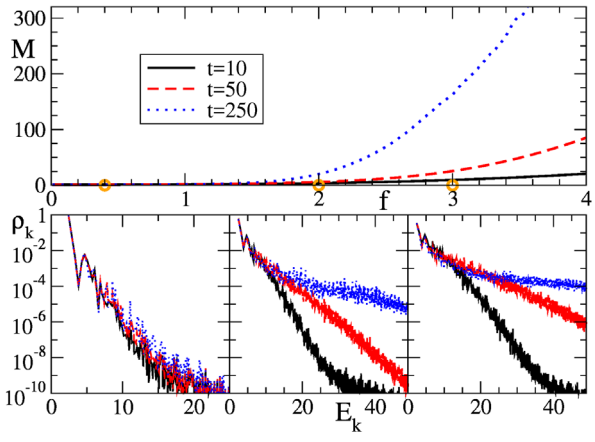

FIG. 3. Top panel shows M as a function of driven force f for linear case ($\beta = 0$). Bottom panels show probability distribution ρ_k, averaged over time interval $\Delta t = 5$, as a function of eigenenergies E_k with $t = 10$ in black solid lines, $t = 50$ in the red (gray) dashed lines, and $t = 250$ in blue (gray) dotted lines. Left, center, and right bottom panels show the cases of $f = 0.4$, 2, and 3, respectively [highlighted with orange (gray) circles in top panel].

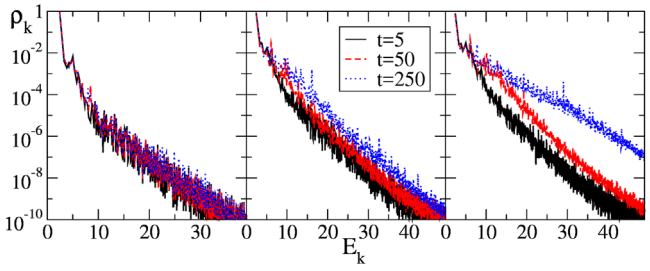

FIG. 4. Same as in bottom panels of Fig. 3 for $f = 0.3$, $\beta = 1.5$ (left panel); $f = 0.5$, $\beta = 5$ (center panel); $f = 1$, $\beta = 5$ (right panel).

energy flow to high energies and the Anderson localization remains robust for weak nonlineary perturbation. This is also well confirmed by a stable in time probability distribution over energies E_k shown in Fig. 4 (left panel). For larger nonlinearity $\beta = 5$ and $f = 0.4$ there appears a growth of M, E with time (Fig. 2). At larger $f = 1$ and $\beta = 5$ there is emergence of energy flow to high energies and increasing probability ρ_k at high energies E_k (Fig. 4, right panel).

The global dependence of average mode number M on driving amplitude f and nonlinearity β is shown in Fig. 5. We see that there is a stability region of small f, β values where the values M remain small even at large times. This region corresponds to the localized insulator phase (I), from the view point of Anderson localization, of quasi-integrable KAM (or laminar) phase from the view point of nonlinear dynamics (or turbulence). Outside of this region we have large values of number of populated states M so that this regime corresponds to the delocalized metallic or turbulence phase (M TB). According to the obtained results we conclude that this quasistable (or insulator) regime ($f < f_c$, $\beta < \beta_c$) (see Fig. 5) is approximately described by the relation

$$f_c r_d/\hbar\omega_x \approx 1.5[1 - \beta_c/(6\hbar\omega_x r_d^2)] \qquad (3)$$

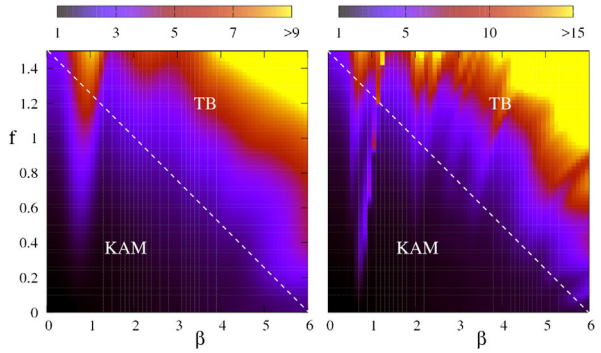

FIG. 5. Number of modes M shown by color (grayness) in the plane of parameters f and β (average is done in the time intervals $100 \le t \le 150$ and $250 \le t \le 300$ in left and right panels, respectively). The approximate separation of KAM or insulator phase (KAM) and delocalized turbulent or metallic phase (TB) is shown by the white line (3).

assuming that $\omega_x \sim \omega_y \sim \omega$. Inside the I region the turbulent Kolmogorov flow of energy to high modes is suppressed by the Anderson localization. At small nonliniarity β we expect a validity of the Kolmogorov-Arnold-Moser theory (KAM) [37,38] leading to a quasi-integrable dynamics and trapping of energy on large length modes. At the same time we should note that the mathematical proof of KAM for nonlinear perturbation of pure-point spectrum of Anderson localization and the GPE (2) still remains an open challenge [18,39,40]. Since our numerical results for the localized KAM phase (see Fig. 5) are obtained at finite times the mathematical prove of existence of finite critical β represents an important problem.

Outside of the stability region (3) a microwave driving transfers the energy flow from low to high energy modes generating the Kolmogorov energy flow. We expect that the energy dissipation and high modes leads to the Kolmogorov spectrum of energy distribution [4,5] over modes. Our results show that the RPA is definitely not valid since its random noisy phases always lead to energy flow to high modes [41]. In contrast, we show that at small amplitudes of a monochromatic driving and small nonlinearity, the Kolmogorov turbulent flow to high modes is defeated by the Anderson localization and the KAM integrability. The transition from the KAM phase to turbulence phase corresponds to the insulator-metal transition in disordered systems with the energy axis corresponding to the spatial distance respectively. The KAM or insulator phase corresponds to a usual observation that a small wind (small f amplitude) is not able to generate turbulent waves. Of course, the original concept of Kolmogorov turbulence had been developed for infinite systems [4,5] but all laboratory experiments are done with finite size systems (e.g., finite size flume in Ref. [42]) as well as numerical simulations [34,35]. Our results for finite systems show that there is a stability domain (see Fig. 5) where the Kolmogorov flow from large to small scales is stopped by the Anderson localization and KAM-integrability effects. The investigations with ultracold atoms will lead to a deeper understanding of this nontrivial phenomenon.

The experimental realization of our system with BEC in a magneto-optical trap corresponds to the experimental conditions described in Ref. [24]. A monochromatic perturbation can be created by oscillations of the center of harmonic potential or effectively by oscillations of the disk position created by the laser beam. We note that the experimental investigations of turbulent cascades in quantum gases become now possible [43] as well as a thermometry of energy distribution in ultracold atom ensembles [44]. The effects of system parameter modulation are now at the beginning of experimental studies [45]. Thus, we hope that the interesting fundamental aspects of nonlinear dynamics and weak turbulence will be tested with cold atom experiments.

Our analysis is done in the frame of GPE, which gives a good approximate description of real many-body quantum system of atoms [32]. Further improvements can be reached

with the multiconfigurational time-dependent Hartree method [46]. However, the experiments with BEC in the described driven Sinai-oscillator trap will allow us to test the validity of these approximate methods for the description of real many-body quantum evolution in the nontrivial regime.

This work was supported in part by the Pogramme Investissements d'Avenir ANR-11-IDEX-0002-02, reference ANR-10-LABX-0037-NEXT (Project THETRACOM).

[1] A. N. Kolmogorov, Dokl. Akad. Nauk SSSR **30**, 299 (1941); **32**, 19 (1941); Proc. R. Soc. Ser. A **434**, 19 (1991); **434**, 15 (1991).
[2] A. M. Obukhov, Izv. AN SSSR Ser. Geogr. Geofiz. **5**, 453 (1941).
[3] V. E. Zakharov and N. N. Filonenko, J. Appl. Mech. Tech. Phys. **8**, 37 (1967).
[4] V. E. Zhakharov, V. S. L'vov, and G. Falkovich, *Kolmogorov Spectra of Turbulence* (Springer-Verlag, Berlin, 1992).
[5] S. Nazarenko, *Wave Turbulence* (Springer-Verlag, Berlin, 2011).
[6] P. W. Anderson, Phys. Rev. **109**, 1492 (1958).
[7] E. Akkermans and G. Montambaux, *Mesoscopic Physics of Electrons and Photons* (Cambridge University Press, Cambridge, England, 2007).
[8] B. V. Chirikov, F. M. Izrailev, and D. L. Shepelyansky, Sov. Sci. Rev. Sect. C **2**, 209 (1981).
[9] S. Fishman, D. R. Grempel, and R. E. Prange, Phys. Rev. Lett. **49**, 509 (1982).
[10] B. V. Chirikov, F. M. Izrailev, and D. L. Shepelyansky, Physica (Amsterdam) **33D**, 77 (1988).
[11] T. Prosen and D. L. Shepelyansky, Eur. Phys. J. B **46**, 515 (2005).
[12] D. Shepelyansky, Scholarpedia **7**, 9795 (2012).
[13] P. M. Koch and K. H. A. van Leeuwen, Phys. Rep. **255**, 289 (1995).
[14] F. L. Moore, J. C. Robinson, C. F. Bharucha, B. Sundaram, and M. G. Raizen, Phys. Rev. Lett. **75**, 4598 (1995).
[15] J. Chabe, G. Lemarie, B. Gremaud, D. Delande, P. Szriftgiser, and J. C. Garreau, Phys. Rev. Lett. **101**, 255702 (2008).
[16] D. L. Shepelyansky, Phys. Rev. Lett. **70**, 1787 (1993).
[17] A. S. Pikovsky and D. L. Shepelyansky, Phys. Rev. Lett. **100**, 094101 (2008).
[18] S. Fishman, Y. Krivolapov, and A. Soffer, Nonlinearity **25**, R53 (2012).
[19] L. Ermann and D. L. Shepelyansky, New J. Phys. **15**, 123004 (2013).
[20] T. V. Laptyeva, M. V. Ivanchenko, and S. Flach, J. Phys. A **47**, 493001 (2014).
[21] T. Schwartz, G. Bartal, S. Fishman, and M. Segev, Nature (London) **446**, 52 (2007).
[22] E. Lucioni, B. Deissler, L. Tanzi, G. Roati, M. Zaccanti, M. Modugno, M. Larcher, F. Dalfovo, M. Inguscio, and G. Modugno, Phys. Rev. Lett. **106**, 230403 (2011).
[23] D. L. Shepelyansky, Eur. Phys. J. B **85**, 199 (2012).
[24] K. B. Davis, M.-O. Mewes, M. R. Andrews, N. J. van Druten, D. S. Durfee, D. M. Kurn, and W. Ketterle, Phys. Rev. Lett. **75**, 3969 (1995).
[25] J. A. Anglin and W. Ketterle, Nature (London) **416**, 211 (2002).
[26] W. Ketterle, Rev. Mod. Phys. **74**, 1131 (2002).
[27] Ya. G. Sinai, Russ. Math. Surv. **25**, 137 (1970).
[28] L. Ermann, E. Vergini, and D. L. Shepelyansky, Phys. Rev. A **94**, 013618 (2016).
[29] E. Wigner, SIAM Rev. **9**, 1 (1967).
[30] O. Bohigas, M. J. Giannoni, and C. Schmit, Phys. Rev. Lett. **52**, 1 (1984).
[31] F. Haake, *Quantum Signatures of Chaos* (Springer, Berlin, 2010).
[32] L. Pitaevskii and S. Stringari, *Bose-Einstein Condensation* (Oxford Univ. Press, New York, 2003).
[33] L. D. Landau and E. M. Lifshitz, *Statistical Physics* (Wiley, New York, 1976).
[34] S. Nazarenko, M. Onorato, and D. Proment, Phys. Rev. A **90**, 013624 (2014).
[35] K. Fujimoto and M. Tsubota, Phys. Rev. A **91**, 053620 (2015).
[36] F. Benvenuto, G. Casati, I. Guarneri, and D. L. Shepelyansky, Z. Phys. B **84**, 159 (1991).
[37] B. V. Chirikov, Phys. Rep. **52**, 263 (1979).
[38] A. J. Lichtenberg and M. A. Lieberman, *Regular and Chaotic Dynamics* (Springer, Berlin, 1992).
[39] J. Bourgain and W.-M. Wang, J. Eur. Math. Soc. **10**, 1 (2008).
[40] S. B. Kuksin, *Hamiltonian PDEs*, in *Handbook of Dynamical Systems*, edited by B. Hasselblatt and A. Katok (Elsvier, Amsterdam, 2006).
[41] RPA gives energy growth at arbitrary small perturbation while our results show that this growth emerges only above a certain chaos border; this is similar to the case of the Chirikov standard map where RPA gives energy growth at any perturbation while due to KAM curves the diffusive growth appears only above the chaos border [37,38].
[42] S. Nazarenko and S. Lukaschuk, Annu. Rev. Condens. Mater. Phys. **7**, 61 (2016).
[43] N. Navon, A. L. Gaunt, R. P. Smith, and Z. Hadzibabic, Nature (London) **539**, 72 (2016).
[44] R. S. Lous, I. Fritsche, M. Jag, B. Huang, and R. Grimm, Phys. Rev. A **95**, 053627 (2017).
[45] V. I. Yukalov, A. N. Novokov, and V. S. Bagnato, Laser Phys. Lett. **11**, 095501 (2014).
[46] O. E. Alon, A. I. Streltsov, and L. S. Cederbaum, Phys. Rev. A **77**, 033613 (2008).